Ali, M.; Ahmed, I.; Ramirez Hoyos, P.; Nasir, S.; Niemeyer, CM.; Mafe, S.; Ensinger, W. (2016). Label-Free Pyrophosphate Recognition with Functionalized Asymmetric Nanopores. Small. 12(15):2014-2021. doi:10.1002/smll.201600160

DOI: 10.1002/ ((please add manuscript number))
Article type: Full Paper

Label-free Pyrophosphate Recognition with Functionalized Asymmetric Nanopores

Mubarak Ali, Ishtiaq Ahmed, Patricio Ramirez, Saima Nasir, Christof M. Niemeyer, Salvador Mafe, and Wolfgang Ensinger*

((Optional Dedication))

Dr. M. Ali, Dr. S. Nasir, Prof. W. Ensinger
Department of Material- and Geo-Sciences, Materials Analysis
Technische Universität Darmstadt
D-64287 Darmstadt, Germany
E-mail: m.ali@gsi.de; m.ali@ca.tu-darmstadt.de

Dr. M. Ali, Dr. S. Nasir
Materials Research Department
GSI Helmholtzzentrum für Schwerionenforschung
D-64291, Darmstadt, Germany

Dr. I. Ahmed, Prof. C. M. Niemeyer
Karlsruhe Institute of Technology (KIT),
Institute for Biological Interfaces (IBG-1)
D-76344 Eggenstein-Leopoldshafen, Germany

Prof. P. Ramirez
Dept. de Física Aplicada
Universitat Politécnica de València
E-46022 Valencia, Spain

Prof. S. Mafe
Dept. de Física de la Terra i Termodinàmica
Universitat de València
E-46100 Burjassot, Spain

Keywords: track-etched nanopores, functionalization, pyrophosphate sensing, current rectification, Nernst-Planck equations, Zn(II)-dipicolylamine complexes

We demonstrate experimentally and theoretically the label-free detection of pyrophosphate (PPi) anion with a nanofluidic sensing device based on asymmetric nanopores. The pore surface is functionalized with zinc complexes based on two di(2-picolyl)amine [bis(DPA)] moieties using carbodiimide coupling chemistry. The complexation of zinc ion is achieved by exposing the modified pore to a solution of zinc chloride to form bis(Zn2+–DPA) complexes.

The chemical functionalization is demonstrated by recording the changes in the observed current–voltage (I–V) curves before and after pore modification. The bis(Zn2+–DPA) complexes on the pore walls serve as recognition sites for pyrophosphate (PPi) anion. The specific binding of PPi inside the confined geometry gives measurable changes in the electronic readout resulting from the modulation of ion flux rectification. The experimental results show that the proposed nanofluidic sensor has the ability to sense picomolar concentrations of PPi anion in the surrounding environment. On the contrary, it did not respond to other phosphate anions, including monohydrogen phosphate, dihydrogen phosphate, adenosine monophosphate, adenosine diphosphate and adenosine triphosphate, even at micromolar concentrations. In all cases, the experimental results are described theoretically by using a model based on the Poisson-Nernst-Planck equations together with the geometrical and electrical single pore characteristics.

1. Introduction

Recently, nanofluidic ion channels and pores have gained remarkable attention as miniaturized sensing devices because of their unique ion transport properties.[1] These nanosensors have been used for the detection of a variety of analytes.[2] The working principle is based on the modulation of transmembrane ion currents and electrical signals originated either by the passage of an analyte through the pore under an applied voltage or on the ligand-receptor interactions occurring when the analyte is introduced in the environment of the ligand-modified pore.

Protein ion channels (e.g. α-hemolysin) allow interfacial chemistry processes controlled with high precision and have frequently been employed for the sensing of analyte molecules.[3] However, they are functional only if embedded in a fragile bilayer. The lipid bilayer/protein nanopore system may be mechanically unstable unless prepared in supported configurations.

Synthetic ion pores fabricated in solid-state materials display several advantages over protein pores concerning stability, control over pore shape and size, possibility of integration into nanofluidic devices, and tailored surface characteristics.[1b,4]

Asymmetric pores prepared through ion-track-technology[5] show some transport properties reminiscent of those in biological ion channels. Track-etched conical pores in polymer membranes exhibit transport characteristics such as ion permselectivity and current rectification due to the carboxylic acid (COOH) groups on the pore surface.[6] Moreover, the pore surface can be easily decorated with specific ligands for detection of particular analyte molecules, e.g., metal ions, small organic molecules, and macro-biomolecules (DNA and proteins).[1a,1c,2b,2c,2h,7]

During the recent years, much attention has been devoted to miniaturize the sensing devices for the selective detection of biologically important anions.[8] Amongst the various phosphate anions, pyrophosphate (PPi) anion plays a vital role in different biological processes.[9] PPi is a small negatively charged ($P_2O_7^{4-}$) analyte produced in the living organisms as a by-product of adenosine triphosphate (ATP) hydrolysis in the cellular system. This anion participates in a variety of enzymatic reactions controlling metabolic and energy transduction processes. The deficiency and an excess of PPi concentration in biological systems results in the deposition of calcium in arteries, referred as Mönckeberg's arteriosclerosis (MA), and the calcium pyrophosphate deposition disease (CPDD), respectively.[10] Moreover, the monitoring of the PPi concentration level is also important in real-time DNA sequencing techniques.[11] The design of a sensing device for the selective detection of PPi under aqueous conditions is therefore a challenge for the scientific community.

To date, a variety of fluorescent and colorimetric chemosensors have been developed for the detection of PPi analyte.[8a-c] The majority of these techniques exploit metal chelator ligands which transduce changes in the corresponding fluorescent or colorimetric signals on binding

with PPi anion. Among the various metal complexes, zinc complexes based on two di(2-picolyl)amine [bis(DPA)] moieties have proved effective binders for the PPi sensing.[7d,8a,8b,12] Recently, Varma and co-workers have reported label-free electrical detections of PPi with a chelator-functionalized field-effect transistor.[13] They have also successfully employed this technique to detect PPi generated during the DNA polymerase reactions.[14]

We demonstrate here the label-free detection of PPi with a nanofluidic sensing device based on a single asymmetric pore. To achieve this goal, the pore surface is chemically functionalized with bis(DPA) ligands via carbodiimide coupling chemistry. Subsequently, the complexation of zinc ions is achieved by exposing the modified pore to a solution of zinc(II). This procedure leads to the formation of bis(Zn^{2+}–DPA) complexes on the pore walls. The Zn(II)-complexes act as recognition sites for the capturing of PPi anions. To demonstrate the success of the chemical functionalization, changes in the transmembrane ion flux are recorded in the form of current–voltage (*I*–*V*) curves before and after pore modification. The single pore is employed for the highly sensitive, specific detection of PPi anion.

2. Results and discussions

Single conical nanopores were fabricated in polyethylene terephthalate (PET) membranes of thickness 12µm *via* asymmetric track-etching technique.[6d] Due to the chemical etching of the latent tracks produced by the heavy ions, carboxylic acid (COOH) groups were generated on the pore surface because of the cleavage of polymeric chains. The exposed COOH groups were available for the covalent attachment of the desired ligands/functional moieties on the nanopore surface under mild conditions.

The chelating ligand bis(DPA)–NH_2 was composed of two di(2-picolyl)amine (DPA) moieties and a terminal amine group. The pore surface COOH groups were covalently

attached with the amine group of the ligand. The attached DPA moieties can then function as binding sites for Zn(II) ion complexation which subsequently enables selective capture of pyrophosphate (PPi) anions. The amine terminated ligand bis(DPA)–NH_2 was synthesized by adopting the reported method with slight modifications (**Figure 1A**).[13] Briefly, the tosylation of the 5-nitro-1,3-bishydroxymethylbenzene (**1**) was achieved by the reaction of *p*-toluene sulfonyl chloride to obtain the compound (**2**). The substitution of tosyl with DPA groups was achieved by reacting the di-(2-picolyl)amine. This resulted in a DPA-nitrobenzene derivative (**3**). The reduction of the nitro groups into an amine was carried out using Pearlman's catalyst ($Pd(OH)_2/C$) to obtain bis(DPA)–NH_2 molecules (**4**).

Figure 1B represents the immobilization of ligand bis(DPA)–NH_2) molecules on the pore surface. For thsi purpose, the pore surface COOH groups were first activated into amine-reactive PFP-esters *via* *N*-(3-dimethylaminopropyl)-*N*′-ethylcarbodiimide/pentafluorophenol (EDC/PFP) coupling chemistry.[15] Subsequently, the PFP-intermediate was covalently coupled with the terminal amine group of the ligand. **Figure 2B** shows the *I–V* characteristics of the single conical pore before and after the immobilization of ligand on the surface. The experiments were performed under symmetric solution conditions and the electrolyte (100 mM KCl) was prepared in 10 mM tric-buffer (pH 8.0). In our electrode configuration, higher (positive) currents were recorded at positive voltages while lower (negative) currents were obtained at negative voltages. The as-prepared (unmodified) conical pore preferentially transported cations from the narrow opening to the wide opening of the cone due to the presence of ionised carboxylate (COO^-) groups and shows current rectification.[6c] The functionalization of ligand molecules resulted in the loss of pore surface charge due to the presence of uncharged DPA moieties. This caused the loss of current rectification (the pore behaved like an ohmic resistor as evidenced from the linear *I–V* curve shown in **Figure 2B(I)**. This clearly confirmed the successful modification of the pore walls with ligand molecules.

After functionalization of the ligand, the complexation of Zn(II) ions with immobilized DPA moieties was achieved by treating the modified pore with an aqueous solution of zinc chloride **(Figure 2A)**. **Figure 2B(II)** shows the *I–V* curves of the modified nanopore prior to and after the complexation of Zn^{2+} ions with DPA moieties on the pore surface. The DPA unit with three nitrogen donors acted as a tridentate ligand and had the ability to form a stable complex with Zn(II) ions compared to other metallic ions.[16] Upon complexation, the bis(Zn^{2+}–DPA) complexes imparted positive charges to the pore surface. As a result the pore became anion-selective, leading to the inversion of current rectification shown in the corresponding *I–V* curve.

The ionic transport through conical nanopores can be described in terms of a Poisson-Nenst-Planck (PNP) model previously developed.[17] The input parameters of the model are the tip (a_T) and basis (a_B) radii of the pore together with the surface charge density σ. The radius of the pore basis was determined by field emission scanning electron microscopy techniques using a PET sample containing 10^7 pores per cm^2, etched simultaneously with the sample containing the single pore. Following this procedure, we obtained base opening radius a_B = 240 nm. The linear curves of Figures 2B(I) and 2B(II) suggest that $\sigma \approx 0$ after the immobilization of ligand on the pore surface. From the fitting of the linear *I–V* curve of the neutral pore, we obtained a tip opening radius a_T = 9 nm. Once the pore radii have been determined, the only free parameter of the model is the surface charge density. The theoretical curves of Figures 2B(III) and 2(IV) reproduced the experimental data by introducing σ = –0.15 e/nm^2 for the as-prepared pore and σ = 0.09 e/nm^2 for the bis(Zn^{2+}–DPA) pore. These values are in agreement with previous results obtained for asymmetric nanopores with different active groups.[18]

After the successful anchoring of bis(Zn^{2+}–DPA) complexes, we studied the sensing capability of the sensor towards phosphate anions, particularly PPi. Due to steric flexibility in the immobilized ligand, the binding sites, *i.e.* Zn^{2+}–DPA units, are organized in such a way that they can selectively capture PPi in contrast to other phosphates (**Figure 3A**). The mass transport through the pore is governed by three main mechanisms: *i*) volume exclusion, *ii*) hydrophobic interactions and *iii*) electrostatic interactions.[19] In the present case, we focus on the electrostatic interaction, in which the detection process is based on the electrical characteristics of the pore walls.[2h,15] It is well-known that ion transport through single conical pores is highly dependent on the surface charges: the direction of current rectification and the permselectivity both depend on the surface charges.[18a,20] Changes in the sign and magnitude of the charge density on the pore surface give significant effects on the ionic selectivity and rectification.

Figure 3B shows the changes observed in the *I*–*V* curves when the modified nanopore was in contact with different PPi concentrations. The sensitivity is an important parameter for designing nanofluidic sensing devices. To this end the Zn^{2+}-chelated pore was exposed to an electrolyte solution having low concentrations ranging from 10 pM to 10 μM of PPi analyte. The selective binding of the PPi anion by the bis(Zn^{2+}–DPA) moieties switched the pore polarity from positive to negative, thus reversing the pore permselectivity and rectification characteristics. The *I*–*V* curve corresponding to concentration 10 pM showed an increase in the positive current from 1.24 to 2.28 nA and a decrease in the negative current from 2.63 to 1.35 nA at voltages +2 V and –2 V, respectively. Furthermore, the increase in the PPi concentration from 100 pM to 100 nM led to a continuous increase in the pore rectification because the number of PPi receptors bound to the immobilized bis(Zn^{2+}–DPA) increased significantly. This fact led to an increase in the magnitude of the (negative) charge density on the pore surface (Figure 1d). Further increase in the PPi concentration from 0.5 to 10 μM did

not induce significant changes in the electrical rectification, indicating the saturation of the pore surface with PPi moieties. The theoretical curves of **Figure 3B** were able to reproduce quantitatively the experimental data of PPi concentration by introducing surface charge densities ranging from –0.03 e/nm^2 to –0.12 e/nm^2 (the conical pore radii are those of Figure 2). Note the agreement between the changes of the charge sign in **Figure 3B** with the different chemical functionalizations in **Figures 2A** and **3A**.

Figure 4 shows the changes observed in the *I*–*V* curves when the bis(Zn^{2+}-DPA)-modified pore was exposed to an electrolyte solution having different phosphates (sodium salts). To this end, 1 μM concentration of monohydrogen phosphate (HPO_4^{2-}), dihydrogen phosphate ($H_2PO_4^-$), adenosine monophosphate (AMP), adenosine diphosphate (ADP), adenosine triphosphate (ATP) and pyrophosphate (PPi) were prepared in 0.1 M KCl (10 mM tric-buffer; pH 8.0). From the *I*–*V* characteristics in **Figure 4a**, we concluded that the bis(Zn^{2+}–DPA)-modified pore displayed a remarkable specificity towards PPi anion: no significant changes were observed in the *I*–*V* characteristics of the single pore exposed to HPO_4^{2-}, $H_2PO_4^-$, AMP, ADP and ATP (phosphates concentrations of 1 μM in the background electrolyte were not recognized by the bis(Zn^{2+}–DPA) moieties). On the contrary, PPi selectively bound with the bis(Zn^{2+}–DPA) moieties under these conditions, imparting negative charge to the pore surface, with the resulting ionic current rectification.

The above measurements proved sensing selectivity and subsequent transduction of specific events on exposure to a specific analyte. This fact clearly showed the validity of our approach to miniaturize the sensing device. Indeed, the changes in the rectified current originated exclusively from the selective PPi binding with bis(Zn^{2+}–DPA) moieties (**Figure 3A**), and were not due to the the adsorption of other anions onto the ligand modified pore.

As in Figures 2 and 3, the theoretical curves of **Figure 4b** were able to reproduce quantitatively the experimental data by introducing the surface charge density as the only parameter (the conical pore radii are those of **Figure 2**). Note again the agreement between the changes of the charge sign in **Figure 3B** with the different chemical functionalizations in Figure 2A and 3A.

Because PPi is a highly negative charged analyte, we wanted to rule out the possibility of physical adsorption on the pore surface. To this end, it was necessary to demonstrate that the switching of pore surface polarity and concomitant changes in the current rectification shown in in **Figure 3** were only due to the selective binding of PPi with the Zn^{2+} ions in the chelator. For this purpose, an additional control experiment was conducted under the same experimental conditions as in **Figure 3** with the bis(DPA)-modified pore (before Zn^{2+} ion complexation). The *I*–*V* curves in **Figure 5** did not show any significant change in the ionic flux across the modified nanopore on exposure to even at higher concentration of phosphate anions (10 μM). These experimental results indicated again that PPi anion can only specifically bind with chelated Zn^{2+} ion in the bis(Zn^{2+}–DPA) moieties immobilized on the pore surface.

3. Conclusions

The label-free specific detection of PPi anion using a nanofluidic sensing device based on a single asymmetric pore was demonstrated experimentally and theoretically. The pore surface was chemically functionalized with zinc complexes based on bis(DPA) moieties by means of carbodiimide coupling chemistry and the feasibility of this functionalization was evaluated by recording the *I*–*V* curves before and after pore modification. The bis(Zn^{2+}–DPA) complexes formed on the pore walls acted as recognition sites, having the ability to detect picomolare concentrations of the PPi anion in the working electrolyte. In contrast, other phosphate anions such as monohydrogen phosphate (HPO_4^{2-}), dihydrogen phosphate ($H_2PO_4^-$), adenosine

monophosphate (AMP), adenosine diphosphate (ADP) and adenosine triphosphate (ATP) could not induce any significant change in the transmembrane ion flux. This indicated the sensitivity and specificity of the proposed nanofluidic sensor towards PPi anion. Moreover, the experimental results were also described theoretically by using a model based on the Poisson-Nernst-Planck equations which incorporated the geometrical and electrical single pore characteristics. We envision that such nanofluidic sensors would readily be used to monitor biological important reactions, e.g., real-time DNA sequencing.

4. Experimental Section

Materials: All the chemicals, including *N*-(3-dimethylaminopropyl)-*N'*-ethylcarbodiimide hydrochloride (EDC, 98%,), pentafluorophenol (PFP, 99+ %,) 5-nitro-m-xylene-α,α'-diol (96%), *p*-toluenesulfonyl chloride (≥ 99 %) , Di-(2-picolyl)amine (97 %), disodium hydrogen phosphate (Na_2HPO_4), sodium dihydrogen phosphate (NaH_2PO_4), adenosine monophosphate (AMP), adenosine diphosphate (ADP), adenosine triphosphate (ATP) and pyrophosphate (PPi) as well as all the solvents were purchased from Sigma-Aldrich, Taufkirchen, Germany, and were used without further purification.

^{1}H and ^{13}C NMR spectra were recorded at 500 and 125 MHz in $CDCl_3$, respectively. High-resolution mass spectra were measured using Finnigan MAT90 mass spectrometer. Analytical TLC (silica gel, 60F-54, Merck) and spots were visualized under UV light and/or phosphomolybdic acid-ethanol. Flash column chromatography was performed with silica gel 60 (70-230 mesh, Merck) and basic aluminum oxide (activated, basic, ~150 mesh, 58 Å, Aldrich).

Polyethyleneterephthalate (PET) membranes (Hostaphan RN 12, Hoechst) of 12 μm thickness were irradiated at the GSI Helmholtz Centre for Heavy Ion Research (GSI, Darmstadt) with Au ions (energy: 11 MeV/u, ion fluence: either single or 10^7 ions cm^{-2}). Subsequently, the ion

tracked PET membranes were further irradiated with UV light from each side for 30 minutes in order to sensitize the latent tracks for the etching process.

Fabrication of conical nanopore: An asymmetric track-etching technique was employed to fabricate the conical nanopores in heavy ion tracked PET membranes.[6d] A custom-made conductivity cell with three chambers was used for the fabrication of single-pore and multipore membranes at the same time. A single-shot membrane and a membrane irradiated with 10^7 ions/cm^2 were placed on both sides of the middle chamber of the conductivity cell and clamped tight. The middle chamber, having apertures on both sides, was filled with an etching solution (9 M NaOH). While the other two chambers were filled with a stopping solution (1 M KCl + 1 M HCOOH). The etching process was carried out at room temperature. During the etching process, a voltage of −1 V was applied across the single ion tracked membrane in order to observe the current flowing through the nascent pore. The current remained zero as long as the pore was not yet etched through. After the breakthrough, a point at which the etchant penetrated across the whole length of membrane, an increase in ionic current was observed. The etching process was terminated when the current had reached a certain value. The etched membranes were then washed first with stopping solution in order to neutralize the etchant, followed by washing with deionized water. The etched membranes were further immersed in deionized water overnight in order to remove the residual salts

*Synthesis of amine-terminated bis(dipicolylamine) [bis(DPA)–NH_2]. Preparation of compound **(2)***: 0.5 N aqueous sodium hydroxide (60 mL) was added to a solution of 5-nitro-m-xylene-α,α'-diol **1** (1.0 g, 5.46 mmol) prepared in THF (40 mL) at 0°C. The mixture was stirred for 1 hour at room temperature. The solution of *p*-toluenesulfonyl chloride (8.3 g, 43.7 mmol in 50 mL of THF) was then added to reaction mixture dropwise at room temperature. After the reaction mixture was stirred at room temperature overnight, ethyl acetate (100 mL) was added. The organic phase was washed with water (3x50 mL) and dried over anhydrous

sodium sulfate. The solvent was then removed under reduced pressure and the residue was purified by silica gel chromatography using a 2:1 to 1:1 mixture of hexane and ethyl acetate to afford pure tosylated compound **2** as colorless oil in 98 % yield (2.62 g, 5.35 mmol). The reaction products were characterized with NMR spectroscopy.

^{1}H NMR (500 MHz, $CDCl_3$): δ (ppm) 2.46 (s, 6H), 5.10 (s, 4H), 7.37 (d, *J* = 8.1Hz, 4H), 7.54 (s, 1H), 7.79 (d, *J* = 8.1Hz, 4H), 8.01 (bs, 2H).

^{13}C NMR (125 MHz, $CDCl_3$): δ (ppm) 21.6, 69.5, 123.1, 127.9, 130.1, 132.5, 133.2, 136.3, 145.6, 148.3.

HRMS-FAB: calcd. for $C_{22}H_{21}NO_8S_2$ $[M+H]^+$ 492.5290, found $[M+H]^+$ 492.5293.

*Preparation of compound **(3)**:* Sodium carbonate (1.06 g, 10.18 mmol) and potassium iodide (1.69 g, 10.18 mmol) were added to a solution of compound **2** dissolved in dried acetonitrile (60 mL). The stirred was for 1 hour at room temperature. Then di-(2-picolyl)amine (DPA) (1.01 mL, 6.10 mmol) was added dropwise to the reaction mixture The mixture was further stirred at room temperature for 5 hours. The solvent was removed under reduced pressure to afford the yellow residue of compound (**3)**. Ethyl acetate (150 mL) and water (150 mL) was then added to the yellow residue. The organic phase was washed with water (3x50 mL) and dried over sodium sulfate. The solvent was removed under reduced pressure and the yellow residue was used in next step without further purification.

1H NMR (500 MHz, CD_3OD): δ (ppm) 3.78 (s, 4H), 3.82 (s, 8H), 7.09 (m, 4H), 7.42 (m, 4H), 7.59 (m, 4H), 7.73 (s, 1H), 8.14 (s, 2H), 8.54 (m, 4H).

13C NMR (125 MHz, CD_3OD): δ (ppm) 57.6, 60.1, 121.9, 122.1, 122.2, 122.9, 135.0, 136.5, 141.3, 148.4, 149.0, 149.2, 158.9.

HRMS-FAB: calcd. for $C_{32}H_{31}N_7O_2$ $[M+H]^+$ 546.6470, found $[M+H]^+$ 546.6477

*Preparation of compound **(4)***: To a solution of compound **3** (200 mg, 0.37 mmol) in 30 mL of methanol, 20 wt% of carbon $Pd(OH)_2$ (500 mg) was added. The flask was purged with a vacuum pump and back-filled with hydrogen using a hydrogen-filled balloon. This was repeated three times and the mixture was stirred under hydrogen atmosphere overnight. The carbon was then filtered and the solvent was removed under reduced pressure. The yellow residue was purified by flash chromatography on basic aluminum oxide column (activated, basic, ~150 mesh, 58 Å, Aldrich) using dichloromethane to 5% methanol in dichloromethane to afford compound (**4**), i.e., bis(DPA)–NH_2 as a light yellow oil in quantitative yield.

^{1}H NMR (500 MHz, CD_3OD): δ (ppm) 3.52 (s, 4H), 3.73 (s, 8H), 6.71 (s, 2H), 6.82 (s, 1H), 7.23 (m, 4H), 7.62-7.78 (m, 8H), 8.41 (m, 4H).

^{13}C NMR (125 MHz, CD_3OD): δ (ppm) 55.7, 57.5, 116.2, 119.9, 120.2, 120.3, 123.8, 123.9124.2, 138.7, 138.8, 140.1, 141.3, 142.1, 149.0, 149.5, 149.9, 150.0, 160.5, 160.9, 161.2.

HRMS-FAB: calcd. for C32H33N7 $[M+H]^+$ 516.6650, found $[M+H]^+$ 516.6658

Functionalization of nanopores: The above-described etching procedure resulted in the generation of carboxyl groups on the surface and inner wall of the nanopore. These carboxyl groups were first converted into amine-reactive pentafluorophenyl esters via pentafluorophenol (PFP) and carbodiimide (EDC) coupling chemistry. For activation, the track-etched single-pore membrane was exposed to an ethanolic solution containing a mixture of 0.1 M EDC and 0.2 M PFP at room temperature for one hour. After washing the activated membrane with ethanol several times, it was further dipped in a solution of bis(DPA)–NH_2 (40 mM) prepared in anhydrous ethanol. The sample was left overnight in bis(DPA)-NH_2 solution. During this reaction period, amine-reactive PFP-esters were covalently coupled with terminal amine group of the ligand**.** Then, the modified pore was washed thoroughly first with ethanol followed by careful rinsing with deionized water. After the successful immobilization

of bis(DPA) moieties, the modified pore was treated with 0.1 mM solution of zinc chloride for the complexation of Zn(II) ions with DPA moieties.

Current–voltage measurements: The as-prepared and modified pores were characterized by measuring the current–voltage (*I–V)* curves before and after the functionalization. To this end, the single-pore membrane was fixed between the two halves of the conductivity cell. An electrolyte (0.1M KCl,) prepared in 10 mM tric-buffer (pH 8.0), was filled on both sides of the membrane. An Ag/AgCl electrode was placed into each half-cell solution and the ionic current flowing through the single pore membrane was measured with a picoammeter/voltage source (Keithley 6487, Keithley Instruments, Cleveland, OH). The ground electrode was placed on the base opening side of the asymmetric pore and the *I–V* curves were recorded by applying a scanning triangle voltage signal from −2 to +2 V across the membrane.

Moreover, various concentrations of pyrophosphate (PPi) and other phosphate anions such as monohydrogen phosphate (HPO_4^{2-}), dihydrogen phosphate ($H_2PO_4^-$), adenosine monophosphate (AMP), adenosine diphosphate (ADP) and adenosine triphosphate (ATP) were prepared in a 0.1 M KCl solution with 10 mM tric-buffer (pH 8.0) and the corresponding *I–V* curves were recorded under symmetric conditions.

Acknowledgements
M.A., S.N. and W.E. acknowledge the funding from the Hessen State Ministry of Higher Education, Research and the Arts, Germany, under the LOEWE project iNAPO. P. R. and S. M. acknowledge financial support by the Generalitat Valenciana (Program of Excellence Prometeo/GV/0069), the Spanish Ministry of Economic Affairs and Competitiveness (MAT2015-65011-P), and FEDER. I.A. and C.M.N. acknowledge financial support through the Helmholtz programme BioInterfaces in Technology and Medicine. The authors are also thankful to Prof. C. Trautmann, Department of Materials Research from GSI, for support with irradiation experiments.

Received: ((will be filled in by the editorial staff))
Revised: ((will be filled in by the editorial staff))
Published online: ((will be filled in by the editorial staff))

[1] a) R. E. Gyurcsanyi, *TrAC, Trends Anal. Chem.* **2008**, *27*, 627-639; b) X. Hou, W. Guo, L. Jiang, *Chem. Soc. Rev.* **2011**, *40*, 2385-2401; c) X. Hou, L. Jiang, *ACS Nano* **2009**, *3*, 3339-3342; dX. Hou, H. C. Zhang, L. Jiang, *Angew. Chem. Int. Ed.* **2012**, *51*, 5296-5307.

[2] a) M. Ali, R. Neumann, W. Ensinger, *ACS Nano* **2010**, *4*, 7267-7274; b) M. Ali, B. Schiedt, R. Neumann, W. Ensinger, *Macromol. Biosci.* **2010**, *10*, 28-32; c) M. Ali, B. Yameen, R. Neumann, W. Ensinger, W. Knoll, O. Azzaroni, *J. Am. Chem. Soc.* **2008**, *130*, 16351-16357; d) D. Fologea, M. Gershow, B. Ledden, D. S. McNabb, J. A. Golovchenko, J. L. Li, *Nano Lett.* **2005**, *5*, 1905-1909; e) S. M. Iqbal, D. Akin, R. Bashir, *Nat. Nanotechnol.* **2007**, *2*, 243-248; f) A. Mara, Z. Siwy, C. Trautmann, J. Wan, F. Kamme, *Nano Lett.* **2004**, *4*, 497-501; g) A. J. Storm, C. Storm, J. H. Chen, H. Zandbergen, J. F. Joanny, C. Dekker, *Nano Lett.* **2005**, *5*, 1193-1197; h) I. Vlassiouk, T. R. Kozel, Z. S. Siwy, *J. Am. Chem. Soc.* **2009**, *131*, 8211-8220.

[3] a) H. Bayley, O. Braha, S. Cheley, L.-Q. Gu, in *Nanobiotechnology*, Wiley-VCH Verlag GmbH & Co. KGaA, Weinheim, Germany, **2005**, pp. 93-112; b) H. Bayley, O. Braha, L. Q. Gu, *Adv. Mater.* **2000**, *12*, 139-142; c) H. Bayley, P. S. Cremer, *Nature* **2001**, *413*, 226-230.

[4] a) C. Dekker, *Nat. Nanotechnol.* **2007**, *2*, 209-215; b) K. Healy, B. Schiedt, A. P. Morrison, *Nanomedicine* **2007**, *2*, 875-897; c) Z. S. Siwy, S. Howorka, *Chem. Soc. Rev.* **2010**, *39*, 1115-1132.

[5] R. Spohr, *Radiat. Meas.* **2005**, *40*, 191-202.

[6] a) Y. E. Korchev, C. L. Bashford, G. M. Alder, P. Y. Apel, D. T. Edmonds, A. A. Lev, K. Nandi, A. V. Zima, C. A. Pasternak, *FASEB J.* **1997**, *11*, 600-608; b) Z. Siwy, P. Apel, D. Dobrev, R. Neumann, R. Spohr, C. Trautmann, K. Voss, *Nucl. Instrum. Methods Phys. Res., Sect. B* **2003**, *208*, 143-148; c) Z. S. Siwy, *Adv. Funct. Mater.* **2006**, *16*, 735-746; d) P. Y. Apel, Y. E. Korchev, Z. Siwy, R. Spohr, M. Yoshida, *Nucl. Instrum. Methods Phys. Res., Sect. B* **2001**, *184*, 337-346.

[7] a) Z. Siwy, L. Trofin, P. Kohli, L. A. Baker, C. Trautmann, C. R. Martin, *J. Am. Chem. Soc.* **2005**, *127*, 5000-5001; b) C. Han, X. Hou, H. Zhang, W. Guo, H. Li, L. Jiang, *J. Am. Chem. Soc.* **2011**, *133*, 7644-7647; c) Q. Liu, K. Xiao, L. Wen, H. Lu, Y. Liu, X.-Y. Kong, G. Xie, Z. Zhang, Z. Bo, L. Jiang, *J. Am. Chem. Soc.* **2015**, *137*, 11976-11983; d) C. Han, H. Su, Z. Sun, L. Wen, D. Tian, K. Xu, J. Hu, A. Wang, H. Li, L. Jiang, *Chem. Eur. J.* **2013**, *19*, 9388-9395; e) G. Perez-Mitta, A. G. Albesa, W. Knoll, C. Trautmann, M. E. Toimil-Molares, O. Azzaroni, *Nanoscale* **2015**, *7*, 15594-15598.

[8] a) H. T. Ngo, X. Liu, K. A. Jolliffe, *Chem. Soc. Rev.* **2012**, *41*, 4928-4965; b) S. Lee, K. K. Y. Yuen, K. A. Jolliffe, J. Yoon, *Chem. Soc. Rev.* **2015**, *44*, 1749-1762; c) S. K. Kim, D. H. Lee, J.-I. Hong, J. Yoon, *Acc. Chem. Res.* **2009**, *42*, 23-31; d) A. E. Hargrove, S. Nieto, T. Zhang, J. L. Sessler, E. V. Anslyn, *Chem. Rev.* **2011**, *111*, 6603-6782.

[9] J. K. Heinonen, Kluwer Academic Publishers, London, U.K., **2001**.

[10] a) A. E. Timms, Y. Zhang, R. G. G. Russell, M. A. Brown, *Rheumatology* **2002**, *41*, 725-729; b) M. Doherty, C. Belcher, M. Regan, A. Jones, J. Ledingham, *Ann. Rheum. Dis.* **1996**, *55*, 432-436; c) K. A. Lomashvili, W. Khawandi, W. C. O'Neill, *J. Am. Soc. Nephrol.* **2005**, *16*, 2495-2500.

[11] M. Ronaghi, S. Karamohamed, B. Pettersson, M. Uhlén, P. Nyrén, *Anal. Biochem.* **1996**, *242*, 84-89.

[12] S. Yang, G. Feng, N. H. Williams, *Org. Biomol. Chem.* **2012**, *10*, 5606-5612.
[13] D. J. Liu, G. M. Credo, X. Su, K. Wu, H. C. Lim, O. H. Elibol, R. Bashir, M. Varma, *Chem. Commun.* **2011**, *47*, 8310-8312.
[14] G. M. Credo, X. Su, K. Wu, O. H. Elibol, D. J. Liu, B. Reddy, T.-W. Tsai, B. R. Dorvel, J. S. Daniels, R. Bashir, M. Varma, *Analyst* **2012**, *137*, 1351-1362.
[15] M. Ali, V. Bayer, B. Schiedt, R. Neumann, W. Ensinger, *Nanotechnology* **2008**, *19*, 485711.
[16] L. Xue, H.-H. Wang, X.-J. Wang, H. Jiang, *Inorg. Chem.* **2008**, *47*, 4310-4318.
[17] a) J. Cervera, B. Schiedt, R. Neumann, S. Mafe, P. Ramirez, *J. Chem. Phys.* **2006**, *124*, 104706; b) P. Ramirez, P. Y. Apel, J. Cervera, S. Mafe, *Nanotechnology* **2008**, *19*, 315707.
[18] a) M. Ali, P. Ramirez, S. Mafe, R. Neumann, W. Ensinger, *ACS Nano* **2009**, *3*, 603-608; b) J. Cervera, A. Alcaraz, B. Schiedt, R. Neumann, P. Ramirez, *J. Phys. Chem. C* **2007**, *111*, 12265-12273.
[19] F. H. J. van der Heyden, D. J. Bonthuis, D. Stein, C. Meyer, C. Dekker, *Nano Lett.* **2007**, *7*, 1022-1025.
[20] a) A. Alcaraz, P. Ramirez, E. Garcia-Gimenez, M. L. Lopez, A. Andrio, V. M. Aguilella, *J. Phys. Chem. B* **2006**, *110*, 21205-21209; b) M. Ali, S. Nasir, P. Ramirez, J. Cervera, S. Mafe, W. Ensinger, *ACS Nano* **2012**, *6*, 9247-9257.

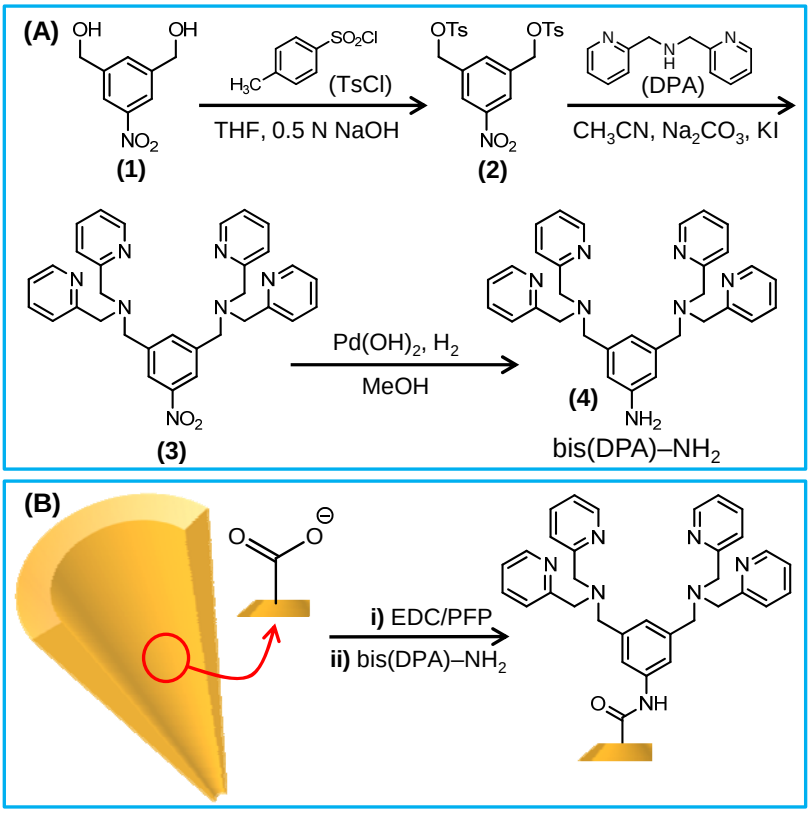

Figure 1. (A) Reaction scheme for the synthesis of bis(DPA)–NH_2. (B) The functionalization of the carboxylic acid groups on the surface of asymmetric nanopore with amine-terminated bis(DPA)–NH_2 molecules via carbodiimide coupling chemistry.

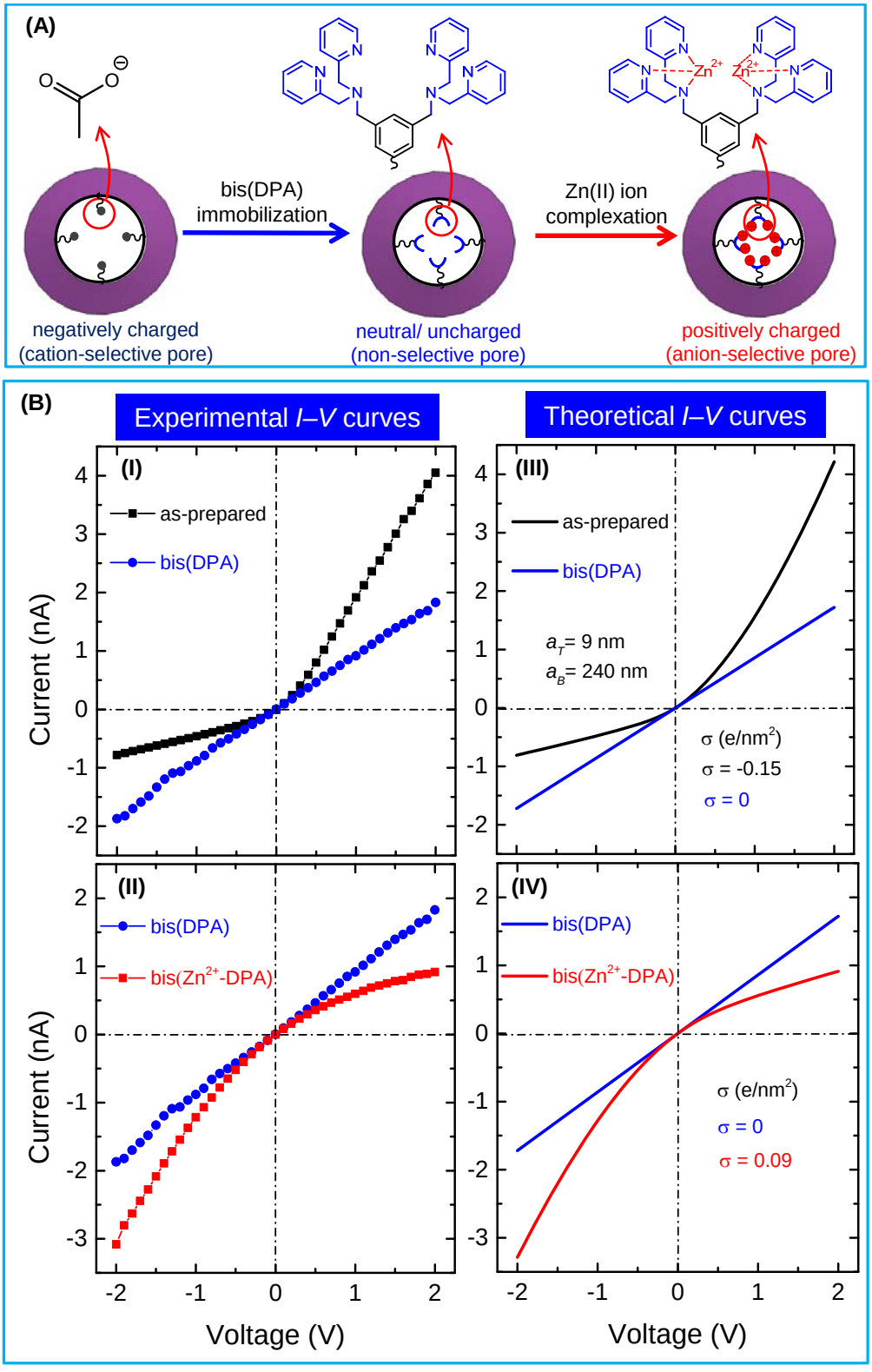

Figure 2. (A) Cartoon representing the changes in pore surface chemistry (B) Experimental and theoretical characterizations: (I) *I–V* curves of the single conical nanopore measured in a 100 mM KCl solution prepared in tric-buffer (10 mM; pH 8.0) before and after the immobilization of amine-terminated chelator [bis(DPA)-NH_2] moieties. (II) *I–V* curves of the chelator-modified nanopore prior to and after the formation of bis(Zn^{2+}-DPA) complexes on the pore surface. (III) and (IV) theoretical *I–V* curves corresponding to the experimental results.

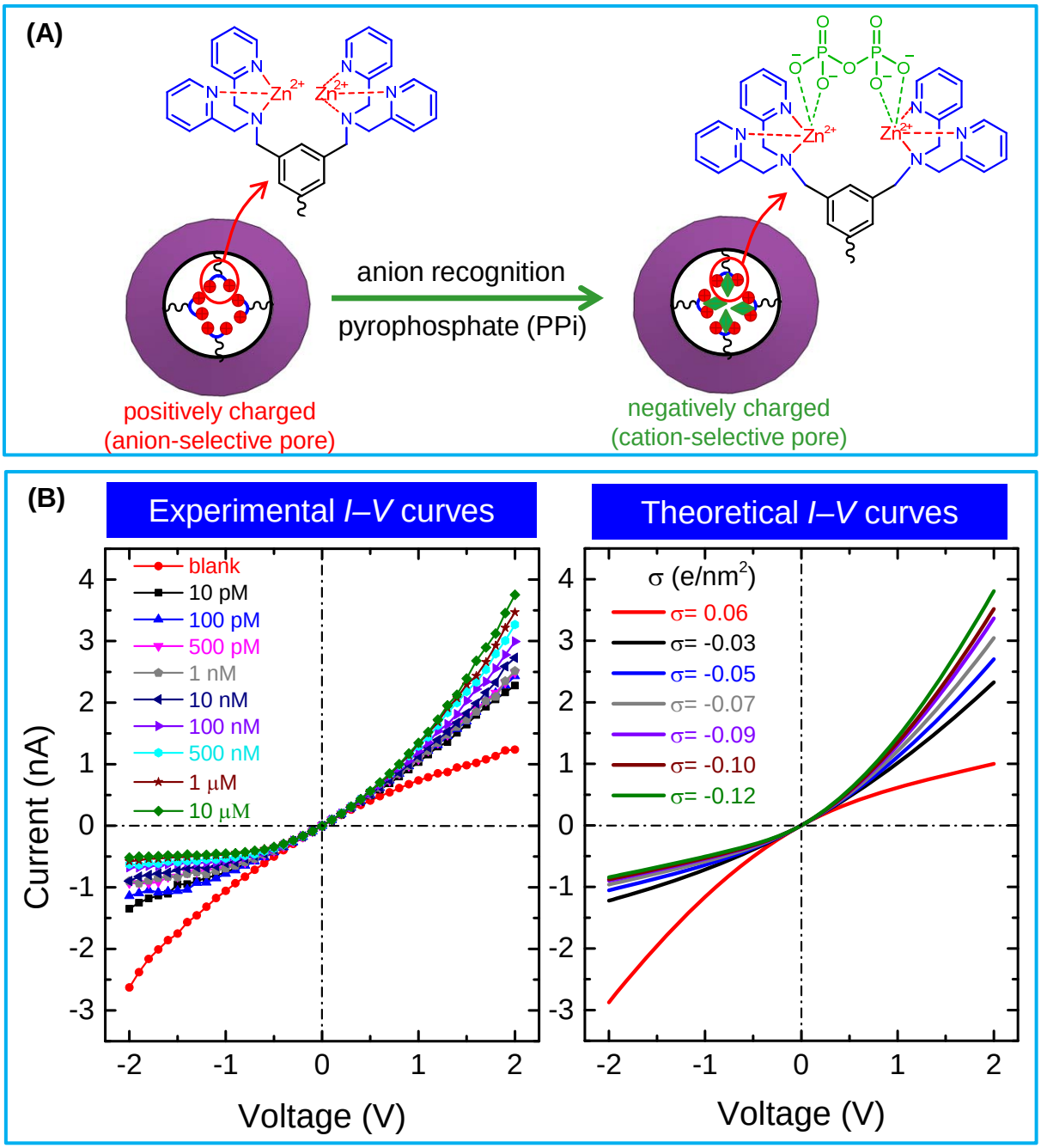

Figure 3. (A) Cartoon representing the changes in pore surface chemistry before and after PPi interaction. (B) Experimental *I–V* curves of the bis(Zn^{2+}-DPA)-modified nanopore measured in 0.1M KCl (pH 8.0) at different PPi concentrations in the range of 10 pM to 10 μM. Theoretical *I–V* curves parametric on the surface charge density.

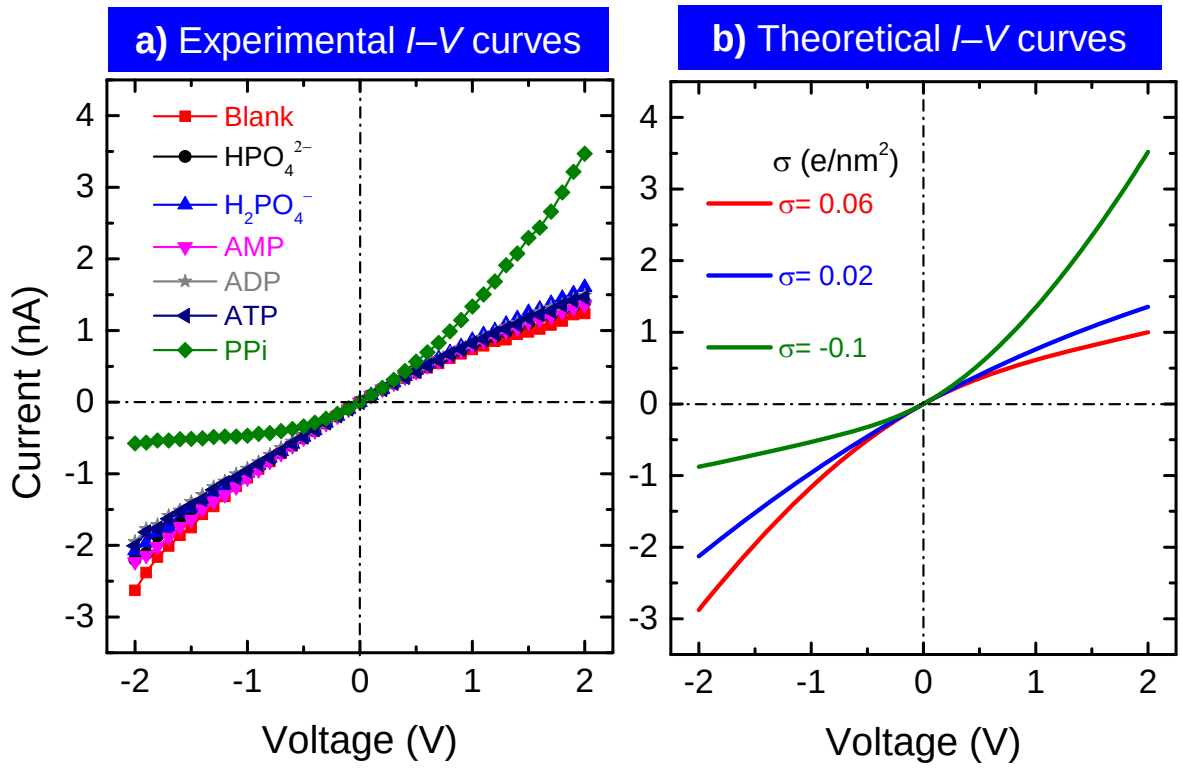

Figure 4. a) *I–V* curves of the bis(Zn^{2+}–DPA)-modified nanopore measured in a 100 mM KCl (pH 8.0) solution in the presence of 1 μM concentration of various phosphates. b) Theoretical *I–V* curves corresponding to the experimental results.

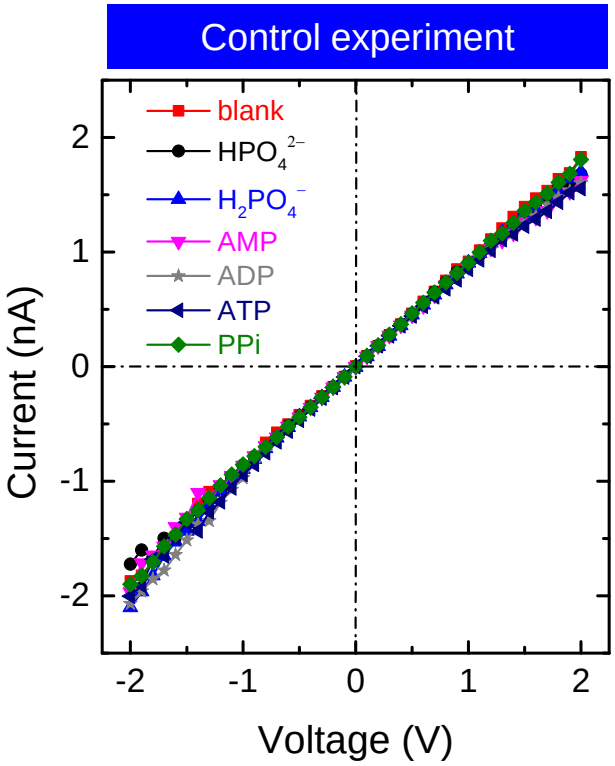

Figure 5. *I–V* curves of the bis(DPA)-modified nanopore measured in a 100 mM KCl (pH 8.0) solution in presence of a 10 μM concentration of various phosphates.

Table of content entry:

A nanofluidic sensor for the sensitive detection of pyrophosphate (PPi) is miniaturized by the chemical functionalization of zinc complexed bis(dipicolylamine) moieties on the pore surface. The specifically capturing of PPi anion in confined environment promotes sensitive changes in the surface charge polarity and the concomitant current rectification characteristic of the asymmetric nanopores.

Keyword: track-etched nanopores, functionalization, pyrophosphate sensing, current rectification, Nernst-Planck equations, Zn(II)-dipicolylamine complexes

Mubarak Ali,* Ishtiaq Ahmed, Patricio Ramirez, Saima Nasir, Christof M. Niemeyer, Salvador Mafe, and Wolfgang Ensinger

Label-free Pyrophosphate Recognition with Functionalized Asymmetric Nanopores